

## Fabrication and field emission properties of boron nanowire bundles

Fei Liu<sup>a</sup>, W.J. Liang<sup>a</sup>, Z.J. Su<sup>a</sup>, J.X. Xia<sup>a</sup>, S.Z. Deng<sup>a</sup>, J. Chen<sup>a</sup>, J.C. She<sup>a</sup>,  
N.S. Xu<sup>a,\*</sup>, J.F. Tian<sup>b</sup>, C.M. Shen<sup>b</sup>, H.-J. Gao<sup>b</sup>

<sup>a</sup> State Key Laboratory of Optoelectronic Materials and Technologies, Guangdong Province Key Laboratory of Display Material and Technology, and School of Physics and Engineering, Sun Yat-sen University, Guangzhou 510275, PR China

<sup>b</sup> Institute of Physics, Chinese Academy of Science, Beijing 100083, PR China

### ARTICLE INFO

PACS:  
81.05.Cy  
81.15.Gh  
79.70.+q

Keywords:  
BNBs  
Chemical vapor deposition  
FE

### ABSTRACT

We have successfully synthesized large-scale crystalline boron nanowire bundles (BNBs) by chemical vapor deposition method. Fe<sub>3</sub>O<sub>4</sub> nanoparticles were used as catalysts spreading on ceramic substrate during the reaction process. The bundles consisted of many thin boron nanowires with a mean diameter of about 25 nm and a length of several micrometers. In addition, boron nanowires are single crystals with an  $\alpha$ -tetragonal structure and grow along [001] orientation. These nanowires have a surface electron affinity of 3.76 eV and a work function of 4.54 eV. A turn-on field of 5.1 V/ $\mu$ m and a threshold field of 10.5 V/ $\mu$ m were found in the nanowire bundles, and stable field emission was recorded at the same time.

© 2008 Elsevier B.V. All rights reserved.

### 1. Introduction

Boron is very special in the periodical table because it has a low density (2.364 g/cm<sup>3</sup>) and a high melting point over 2300 °C, as well as its unique chemical and physical properties [1–7]. Hence study on the boron materials has become more and more attractive during the past ten years. In field emission (FE) area, boron quasi one-dimensional nanostructures are considered as a good cold cathode nanomaterial because they have high conductivity, high aspect ratios and excellent performance in harsh conditions. Although there exist several methods investigating on the synthesis of amorphous or crystalline boron nanowires in recent years [8–13], no reports on the boron nanowire bundles (BNBs) have been found until now. Moreover, little attention [14–16] has been paid to the research on their FE properties and work function though it is especially important for the practical application of field emission display (FED).

In this paper, we report on the synthesis of large-scale crystalline boron nanowire bundles with a mean diameter of about 25 nm by chemical vapor deposition method for the first time. The morphology, structure and the composition of the BNBs were investigated by means of scanning electron microscopy (SEM), transmission electron microscopy (TEM) and electron energy loss spectroscopy (EELS). Their FE performance and work function are investigated in detail. The possible growth mechanism is also proposed here.

### 2. Experimental

Large-scale BNBs were grown using chemical vapor deposition method in a single-stage furnace developed in our group [17]. B<sub>2</sub>O<sub>3</sub> powders (99.99%), boron powder (99.99%) and iron powder (99.99%) were grounded together, and their mass ratio was 1:2:1. Then these powders were loaded to an alumina boat as source materials. Fe<sub>3</sub>O<sub>4</sub> nanoparticles with diameter less than 10 nm were synthesized by high-temperature solution phase reaction method and spread over the ceramic substrate (95% Al<sub>2</sub>O<sub>3</sub>) as the catalysts.

To fabricate crystalline BNBs, firstly, the temperature of the middle reaction region was increased to 400 °C and kept for 30 min. Secondly, when the temperature of reaction region was increased to 1000–1100 °C, the alumina boat loaded with source materials was transferred to the high-temperature zone immediately. The growth lasted for 2–4 h under a constant flow of argon (~25–30 sccm). The reaction pressure was  $1 \times 10^5$  Pa through the process. When the reaction was finished, dark brown or black thin film was found on the surface of the substrate.

A field emission scanning electron microscope (XL-SFEG, FEI Corp.) was used to observe the morphologies of BNBs. Transmission electron microscopy (Tecnai-20, PHILIPS) and high-resolution transmission electron microscopy (HRTEM) (Tecnai F20, FEI Corp.) were used to obtain low-resolution and high-resolution images of the samples, respectively. Measurements on the field emission properties and the work function of BNBs were performed on the home-made field emission analysis and measurement facility and the commercial Omicron VT-AFM system equipped with ultraviolet photoelectron spectroscopy (UPS), respectively.

\* Corresponding author.

E-mail addresses: [stxns@mail.sysu.edu.cn](mailto:stxns@mail.sysu.edu.cn), [liufei@mail.sysu.edu.cn](mailto:liufei@mail.sysu.edu.cn) (N.S. Xu).

### 3. Results and discussion

Fig. 1 shows large-area BNBs lying on a polycrystalline ceramic substrate after a growth time of 2–4 h. Typical SEM image of BNBs is shown in Fig. 1A. The length of the BNBs is about 5–6  $\mu\text{m}$  and their outer diameter is about 1–2  $\mu\text{m}$ . The magnified SEM image of BNBs is given in Fig. 1B, in which one can observe that all the nanowire bundles consisted of many thin boron nanowires. It is also observed that the nanowires are aligned and parallel to each other in the bundles. In addition, these nanowires are joined tightly together in the bundles. When we carefully moved the BNBs with the tweezers, more detailed morphology may be shown as in Fig. 1C. These thin boron nanowires have a uniform morphology, and their mean diameter is about 25 nm. The aspect ratio of boron nanowire is over 200, which is useful for field emission.

In our previous work, we reported the growth of aligned boron nanowire arrays on silicon (001) substrates where the aligned mechanism is attributed to the steric overcrowding [18]. The growth mechanism of BNBs may be a little different from the aligned boron nanowire arrays, which is proposed as follows. Firstly, parallel boron nanowires are obtained on a ceramic substrate at the beginning of the growth, which results from the steric overcrowding as described in Ref. [18]. Secondly, with the processing of the growth, many discrete areas of boron nanowire arrays gradually formed because there are many rough grain boundaries existing on the ceramic substrate [19]. These aligned boron nanowires in these discrete areas cannot form the continuous film because of the restriction of the boundaries and have no way to stand vertically on the substrate as they do on the silicon substrate during the subsequent process. Finally, these parallel nanowires are pushed to lie on the substrate due to the function of gravity according to the theory in Ref. [19], and the BNBs are produced.

High-resolution TEM technique was applied to investigate the crystalline structure of the BNBs. A typical TEM image of the boron nanowires is shown in Fig. 2A. It is found that the morphology of nanowires is rather uniform and they almost have similar diameters and lengths, which is in agreement with the

SEM results in Fig. 1C. Fig. 2B shows the HRTEM image of a boron nanowire in the bundles. From the HRTEM image, it is found that the boron nanowire has clear lattice fringes and the spacing  $d$  between the adjacent (002) growth planes is 5.06 Å. In the inset, sharp diffraction spots are found in the selected area electron diffraction (SAED) pattern, which proves that the boron nanowires are well crystalline. The growth orientation of these boron nanowires is [001], which conforms to the data of the Joint Committee for Powder Diffraction Standards (JCPDS) card no. 73–0511. Combined with the SAED and TEM data, it is concluded that the BNBs consisted of single-crystal boron nanowires with the  $\alpha$ -tetragonal structure. To determine the composition of the nanowires, the EELS technique was used, and the typical spectrum is given in Fig. 2C. Only boron element is monitored in the EELS spectrum, which confirms that the as-grown nanowires are pure boron nanowires. We also determined the diameter distribution of 400 boron nanowires in the bundles, and the corresponding histogram is provided in Fig. 2D. One can see that the diameter of the boron nanowire ranges from 10 to 60 nm, and their mean diameter is 25 nm. In addition, it is also seen that the proportion of nanowires with a diameter between 20 and 40 nm is over 60%. The good uniformity in morphology and well-crystalline structure of the BNBs is important for a cold cathode material considering the requirement of the uniformity of the field emission.

Since work function is an importance factor affecting the emission properties of the as-prepared BNBs film according to the classical FN theory [20], its measurement was carried out before field emission. Ultraviolet photoemission spectroscopy is an effective way to measure the work function of thin film. The typical UPS spectrum of the BNBs is shown in Fig. 3. In order to obtain more accurate values, the low kinetic energy cutoff is magnified by 10 times. In the measurement, the as-prepared sample was biased with 0.5 V to overcome the influence of the analyzer's work function and ensure that all the electrons from the valence band can be collected. By linearly extrapolating the emission onset edges to zero intensity at both the low kinetic energy cutoff and the high kinetic end, we can obtain the spectral widths ( $W_{\text{spectra}}$ ) of the BNBs film. Following this method, the width of the whole spectrum is calculated to be about

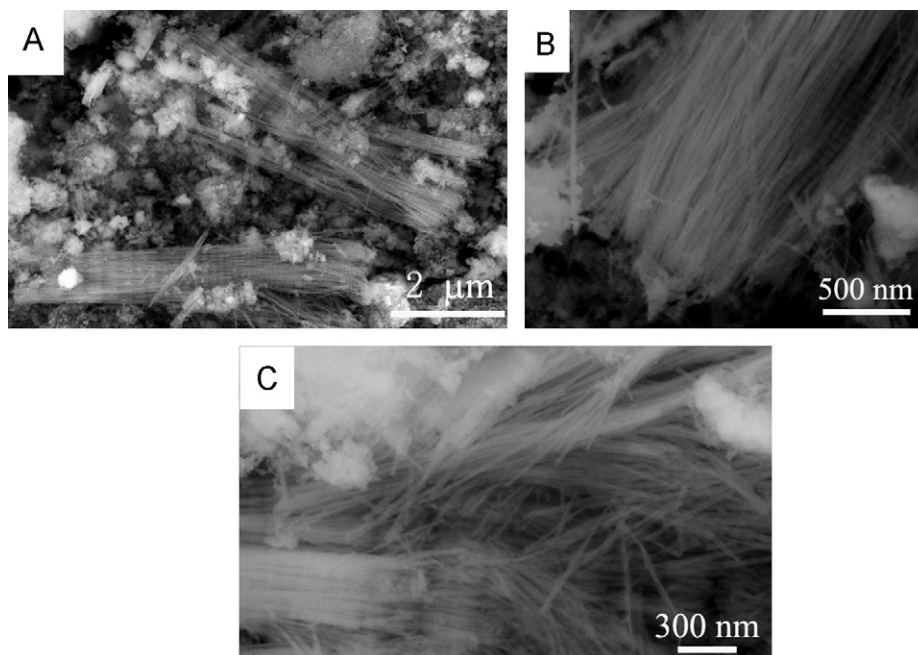
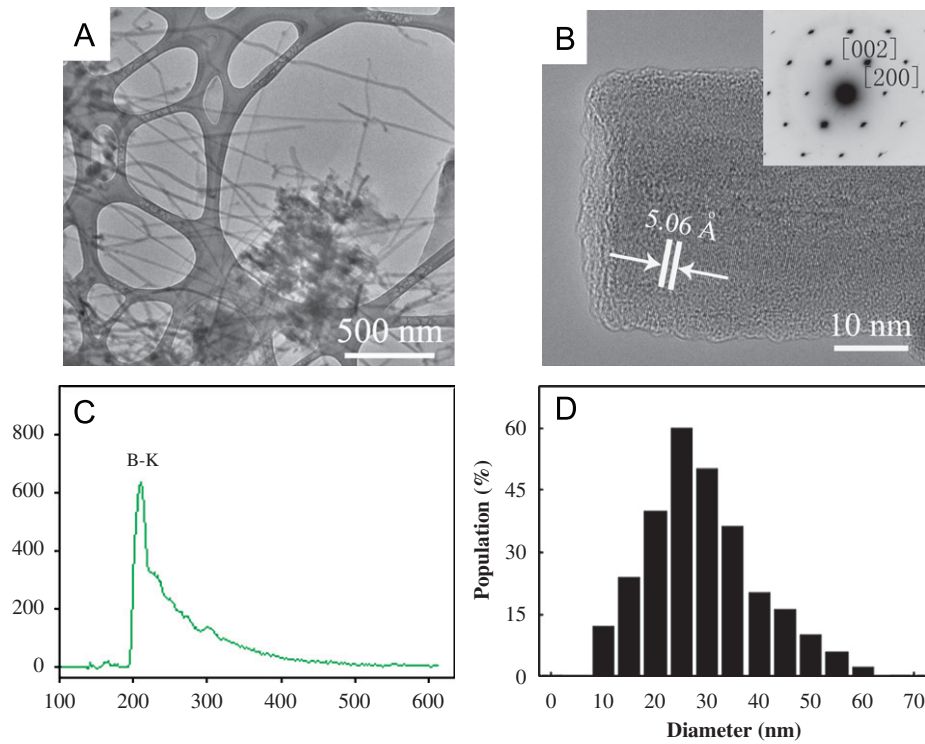
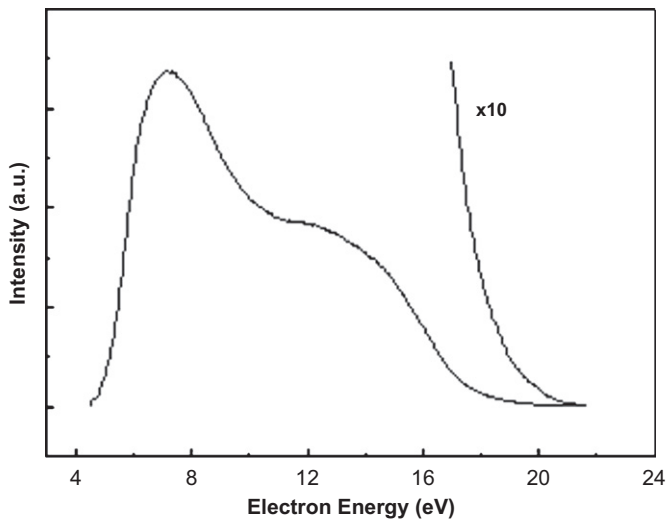


Fig. 1. SEM images of BNBs: (A) Typical SEM image of large-area BNBs, (B) The side view of BNBs and (C) Magnified image of the BNBs.



**Fig. 2.** TEM and HRTEM images taken from BNBs. (A) Typical TEM image of BNBs. (B) HRTEM image of a boron nanowire in the bundle. The inset is the corresponding SAED pattern. (C) The EELS spectrum of a typical boron nanowire. (D) The diameter distribution histogram of the boron nanowire in the bundles.



**Fig. 3.** The representative UPS spectrum of BNBs.

15.9 eV. The surface electron affinity of the sample can be calculated by the relation given below [21]

$$\chi = h\nu - E_g - W_{\text{spectra}}$$

where  $\chi$  and  $E_g$  are the surface electron affinity and the energy band gap of the BNBs film, respectively. And  $h\nu = 21.2$  eV, which is the radiation energy of He I line used in this measurement. For simplicity, we adopt the same energy gap of the sample as that of bulk boron, which is 1.56 eV [1,22]. Then the corresponding  $\chi$  value is calculated to be 3.76 eV for the sample. If the as-prepared BNBs are assumed to be pure and no contamination energy level exists in the energy gap, the work function of the sample should be calculated according to the equation:  $\phi = \chi + E_g/2$ . Through this

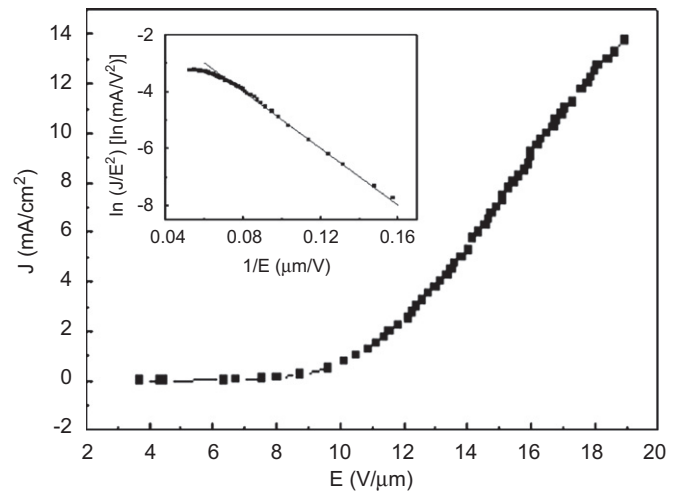


**Fig. 4.**  $J$ - $E$  curve from large-area BNBs film. The inset is the FN plots of the sample.

way, the work function of the sample is determined to be 4.54 eV. The surface electron affinity of the BNBs is low and good for field emission nanomaterials. Moreover, in our recent studies, it is found that the work function value of the BNBs can be adjusted to be lower by doping some elements such as carbon, phosphor and magnesium into the nanowires, which will benefit the FE application.

Field emission measurements were performed on the BNBs to explore the possibility of the bundles in FE applications. A typical curve of the emission current density versus applied electrical field is given in Fig. 4. It is indicated that the turn-on field (defined as the electric field for  $J = 10 \mu\text{A}/\text{cm}^2$ ) of the sample is 5.1 V/ $\mu\text{m}$  and the threshold field (defined as the electric field for

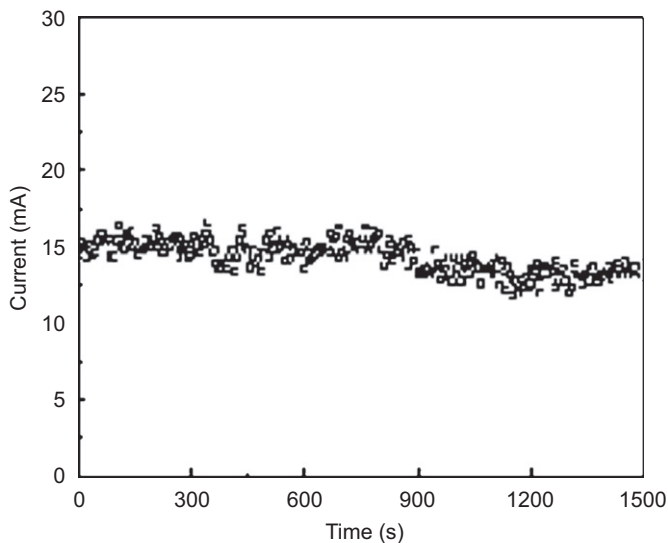


Fig. 5. Typical emission stability curve of BNBs film at high current density.

$J = 1 \text{ mA/cm}^2$ ) is found to be  $10.5 \text{ V}/\mu\text{m}$ . When the electrical field was increased to  $19 \text{ V}/\mu\text{m}$ , the emission current density reached  $14 \text{ mA/cm}^2$ . Moreover, the saturation tendency of the emission current was not observed in the whole measurement. The measured results suggest that the FE behaviors of the BNBs can be comparable to the best results from other nanowires with excellent FE properties [23–26].

The Fowler–Nordheim (FN) equation is used to calculate the F–N plot of the FE properties of our samples and is shown in the inset of Fig. 4. According to the FN theory, the relationship between current density  $J$  and applied electric field  $E$  can be described as follows [20]:

$$J = A \left( \frac{\beta^2 E^2}{\phi} \right) \exp \left( \frac{-B\phi^{3/2}}{\beta E} \right)$$

where  $A = 1.57 \times 10^{-10} \text{ (AV}^{-2} \text{ eV)}$ ,  $B = 6.83 \times 10^9 \text{ (Vm}^{-1} \text{ eV}^{-3/2})$  and  $\phi$  is the work function of the sample, which adopts the value of  $4.54 \text{ eV}$  obtained in our UPS measurement. The enhancement factor  $\beta$  is calculated to be about 1300, which is high enough for emission applications. The linearity of the FN plots suggests that the emission mechanism of the BNBs agrees with the FN theory well.

Finally, we investigate the emission stability behaviors of BNBs at high emission current because of which is another crucial parameter for the practical application of cold cathode nanomaterials. The representative emission stability curve is given in Fig. 5. The electrical field was fixed at about  $17 \text{ V}/\mu\text{m}$  and the whole measurement lasted for 2.5 h. It is found that BNBs exhibit a stable field emission at a high current of  $10 \text{ mA}$  and the fluctuation of emission current is less than 9.5% through the continuous emission operation. Combining the low threshold field behaviors of BNBs with their good stability performance in high current, it is suggested that they can be a kind of good candidate as field emitters.

#### 4. Conclusions

In summary, the BNBs have been successfully prepared on ceramic substrate by way of chemical vapor deposition for the first time. These bundles consisted of many single crystalline boron nanowires growing along  $[001]$  direction, whose diameters almost range from 20 to 40 nm. The as-prepared BNBs have a surface electron affinity of  $3.76 \text{ eV}$  and a high field enhancement factor over 1300. Their threshold electrical field is  $10.5 \text{ V}/\mu\text{m}$ , and they can keep stable emission at a high current density of about  $14 \text{ mA/cm}^2$ . Moreover, the fluctuation of emission at  $10 \text{ mA}$  is less than 9.5% in 2.5 h continuous operation measurement. All these experimental results suggest that the BNBs could have a promising future in FE fields.

#### Acknowledgement

This work is supported by the National Basic Research Program of China (973 Program, Grant no. 2007CB935500, 863 Program, Grant no. 2007AA03Z305, National Nature Science Foundation of China, Grant no. 50802117), the National Joint Science Fund with Guangdong Province (Grant nos. U0634002 and U0734003), the Doctoral Foundation of Education Ministry of China (Grant no. 20070558063), the Science and Technology Department of Guangdong Province, the Education Department of Guangdong Province, and the Science and Technology Department of Guangzhou City.

#### References

- [1] V.I. Matkovich (Ed.), Boron and Refractory Borides, Springer, New York, 1977.
- [2] R.J. Brotherton (Ed.), Progress in Boron Chemistry, Pergamon Press, 1970.
- [3] R.M. Adams (Ed.), Boron, Metallo-Boron Compounds and Boranes, Interscience, New York, 1964.
- [4] D. Emin, Phys. Today 20 (1987) 55.
- [5] J.A. Kohn (Ed.), Boron Synthesis, Structure, and Properties, New York, 1973.
- [6] I. Boustani, A. Quandt, E. Hernandez, A. Rubio, J. Chem. Phys. 110 (1999) 3176.
- [7] A. Gindulyte, W.N. Lipscomb, L. Massa, Inorg. Chem. 37 (1999) 6544.
- [8] Yiyang Wu, Benjamin Messer, Peidong Yang, Adv. Mater. 13 (2001) 1487.
- [9] Liming Cao, Ze Zhang, Liling Sun, et al., Adv. Mater. 13 (2001) 1701.
- [10] Liming Cao, Kersten Hahn, Yiqian Wang, et al., Adv. Mater. 14 (2002) 1294.
- [11] X.M. Meng, J.Q. Hu, Y. Jiang, C.S. Lee, S.T. Lee, Chem. Phys. Lett. 370 (2003) 825.
- [12] Q. Yang, J. Sha, J. Xu, D.R. Yang, et al., Chem. Phys. 379 (2003) 87.
- [13] Y. Zhang, H. Ago, M. Yumura, T. Komatsu, et al., Adv. Mater. 11 (2002) 2806.
- [14] X.J. Wang, J.F. Tian, T.Z. Yang, L.H. Bao, C. Hui, F. Liu, H.J. Gao, et al., Adv. Mater. 19 (2007) 4480.
- [15] D.W. Wang, J.G. Lu, C.J. Otten, W.E. Buhro, Appl. Phys. Lett. 83 (2003) 5280.
- [16] K. Kirihara, Z. Wang, K. Kawaguchi, K. Kimura, et al., Appl. Phys. Lett. 86 (2005) 212101.
- [17] F. Liu, P.J. Cao, H.J. Gao, et al., J. Cryst. Growth 274 (2005) 126.
- [18] F. Liu, J.F. Tian, H.J. Gao, N.S. Xu, et al., Adv. Mater. 20 (2008) 2609.
- [19] P.J. Cao, Y.S. Gu, F. Liu, H.J. Gao, et al., Appl. Phys. A 80 (2005) 195.
- [20] R.H. Fowler, L.W. Nordheim, Proc. R. Soc. London, Ser. A 119 (1928) 173.
- [21] M.C. Benjamin, M.D. Bremser, T.W. Weeks, et al., Appl. Surf. Sci. 104/105 (1996) 455.
- [22] K.H. Hellwege (Ed.), Landolt–Bornstein Numerical Data and Functional Relationships in Science and Technology, New Series, Springer, Berlin, 1983.
- [23] J.C. She, S. An, N.S. Xu, et al., Appl. Phys. Lett. 90 (2007) 073103.
- [24] Han. Zhang, Jie Tang, Lu-Chang Qin, et al., Adv. Mater. 18 (2006) 87.
- [25] N.S. Ramgir, I.S. Mulla, D.S. Joagb, et al., Appl. Phys. Lett. 88 (2006) 042107.
- [26] Y. Yu, C.H. Jin, L.M. Peng, et al., J. Phys. Chem. B 109 (2005) 18772.